# INVERSE ANALYSIS OF STEADY HEAT CONDUCTION WITH  HEAT GENERATION FOR  A HOLLOW CYLINDER

تحليل نظرى معكوس لتوصيل حرارى مستقر مع توليد حرارى لاسطوانة مجوفة

Mohammed Mosaad
Mechanical  Engineering Department, Faculty of Engineering
Mansoura University, Egypt 35516

ملخص :
هذا البحث يتقدم تحليلاً نظرياً معكوساً لحساب التوزيع المستقر ثنائي الابعاد لدرجات الحرارة
في جدم اسطوانة مجوفة تتولد فيه   حرارة  بانتظام ، وذلك  باستخدام توزيع درجة الحرارة
والفيض الحرارى عند  سطح الا سطوانة الخارجى ، والتى تكون فى صورة دوال مستمرة فى
الاحداثى المحورى. الحل   العام الناتج لتوزيع درجات الحرارة حل مريح ومضبوط، كما ان ذو
كفاءة عالية ايضاً عند الظروف الحدية ذات التغير المحورى الحاد (steep axial variation).
وقد امكن التوصل ال صورة مختلفة للحل   وذلك عند استخدام الظروف الحدية  المناظرة على
السطح الداخلى للاسطوانة المجوفة. هذا وقد تم  التحقق من صحة الحل العام وذلك من مقارنتة
مع حل معلوم مضبوط. كما يعتبر هذا الحل ذو اهمبة تطبيقية .

## ABSTRACT

    This work is concerned with the inverse analysis of estimating
two dimensional steady state temperature distribution in a hollow
cylinder wall involving uniform internal heat generation,   by
utilizing the axial distribution of  temperature and that of heat
flux at the outside surface of the cylinder; both are functions of
the axial coordinate. Different version of the solution has also
been found by utilizing the corresponding two boundary conditions
specified at the inner surface of the hollow cylinder. Exactness and
validity of the present solution have been checked up by comparison
with exact solutions. The general solution is capable to accommodate
boundary conditions data of sharp axial variation. The method may
also be of a considerable practical interest, however, for some
steady heat transfer investigations using a circular test tube.

## 1. INTRODUCTION

    In heat transfer studies surface temperature and heat flux are
important  quantities  which  should  accurately  be  estimated.
Therefore, in some steady heat transfer experiments using a circular
test tube with  significant axial variation in wall temperature
and/or heat flux due to the nature of the investigated phenomenon,
it may be necessary to estimate the 2-dimensional temperature field
of the tube wall in order to evaluate accurately the axial
distribution of heat flux, and temperature at the  inner tube
surface (the effective heat transfer surface), however, from only
some corresponding measurements at  the outer surface. This  problem
is not considered a classical boundary value problem  characterizing
by 4 boundary conditions; with 2 for each coordinate, however, it is
identified as inverse problem in heat conduction literatures [1].
The inverse  problems  are  classified  to  steady  and  transient
problems [2].

    In recent  years, there has been  considerable interest in the
solution of  transient inverse problems. Most of those studies have
been performed numerically (e g, [3-5]).   while the analytic ones
(e g, [6,8])  were  scarce  and  usually  restricted  to  the
one-dimensional case due to difficulty of a multi-dimensional
solutionn [6,9].

In our previous work [10], steady-state, two-dimensional, heat conduction problem from the inverse type has been analyzed for a hollow cylinder wall, by following a similar way to the analysis of an inverse problem of transient, one-dimensional heat conduction derived by Burggraf [7] for a hollow cylinder in time and radial coordinates. The similarity between the two analyses lies mainly in that the axial variable in the steady solution plays the role of the time variable in the transient problem solution.

However, it is important to point out that our previous solution [10] is not appropriate to treat this kind of the inverse problems, if there is heat generation in the cylinder wall. Furthermore, it is limited to the case of being the two boundary conditions, required for the solution, are specified at the outer surface of the hollow cylinder. Therefore, the main goal of the present paper is to estimate the two-dimensional steady-state temperature filed of a hollow cylinder wall involving internal heat generation, by utilizing the axial distributions of temperature and heat flux at the outer or the inner surface of the cylinder; both are given as continuous functions of the axial coordinate.

## 2. ANALYSIS

Figure 1 describes an inverse problem of steady heat conduction with internal heat generation in a hollow cylinder wall. This type of the inverse problems is characterized by two boundary conditions: the temperature and the radial heat flux; both are specified at the outer surface (cf. Fig. 1a) or at the inner surface (cf. Fig. 1b) as known continuous and differentiable functions of the axial coordinate y. The boundary conditions at the two radial planes (r,0) and (r,L) are unknown. Our main goal is to evaluate the (r,y) field of temperature in the cylinder wall.
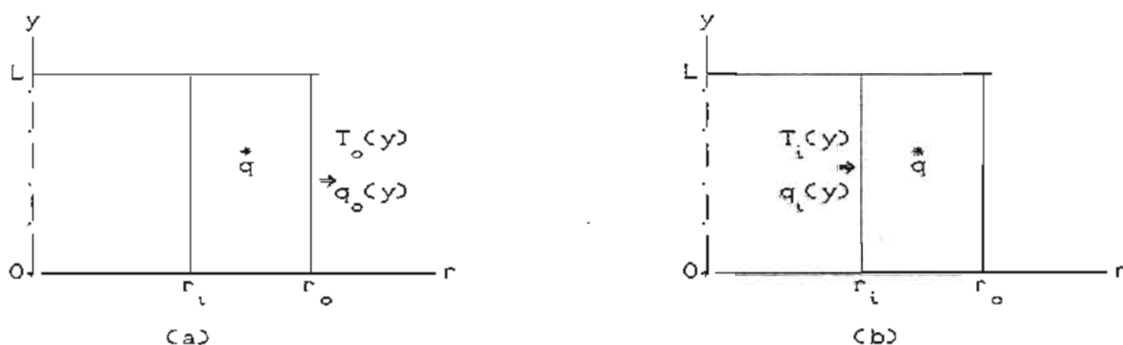


Fig. 1  Problem description

### 2.1 ANALYSIS OF PROBLEM (1a)

If uniform internal heat generation and constant thermal conductivity are assumed, problem (1a) may be modeled by

$$\frac{\partial^2 T}{\partial r^2} + \frac{1}{r}\frac{\partial T}{\partial r} + \frac{\partial^2 T}{\partial y^2} + \frac{\dot{q}}{k} = 0; \qquad T(r_o,y) = T_o(y), \qquad q_r(r_o,y) = q_o(y). \qquad (1)$$

where $T_o(y)$ and $q_o(y)$ are the temperature and radial heat flux at the outer surface, respectively, which should be known continuous and differentiable functions of the axial coordinate $y$ in the interval: $0 \le y \le L$. $\overset{*}{q}$ is the volumetric heat generation rate.

By the superposition principle, the solution of problem (1) may be assumed to be

$$T(r,y) = \psi(r,y) + \phi(r). \tag{2}$$

such that $\phi(r)$ satisfies the one-dimensional problem :

$$\frac{d^2\phi}{dr^2} + \frac{1}{r}\frac{d\phi}{dr} + \frac{\overset{*}{q}}{k} = 0, \qquad \phi(r_o) = 0, \qquad \frac{d\phi}{dr}\bigg|_{r_o} = 0. \tag{3}$$

and $\psi(r,y)$ satisfies the two-dimensional problem :

$$\frac{\partial^2\psi}{\partial r^2} + \frac{1}{r}\frac{\partial\psi}{\partial r} + \frac{\partial^2\psi}{\partial y^2} = 0, \qquad \psi(r_o,y) = T_o(y), \qquad \frac{\partial\psi}{\partial r}\bigg|_{r_o} = -\frac{q_o(y)}{k} \tag{4}$$

The solution of problem (3) is found to be

$$\phi(r) = \frac{\overset{*}{q}r_o^2}{4k}\left[1 - (\frac{r}{r_o})^2 + \ln(\frac{r}{r_o})^2\right]. \tag{5}$$

However, the solution of problem (4) can be obtained by following analysis procedure parallel to that presented in reference [11]. This solution is found as :

$$\psi(r,y) = \left[T_o(y) - \frac{r}{k}\ln(\frac{r}{r_o})q_o(y)\right] + \sum_{n=1}^{\infty} A_n(r)\frac{d^{2n}T_o(y)}{dy^{2n}} + \frac{1}{k}\sum_{n=1}^{\infty} B_n(r)\frac{d^{2n}q_o(y)}{dy^{2n}} \tag{6a}$$

where $A_n(r)$ and $B_n(r)$ are r-dependent functions. The leading terms of $A_n(r)$ are :

$$A_o(r) = 1, \qquad A_1(r) = \frac{r_o^2}{4}\left[1 - (\frac{r}{r_o})^2 + 2\ln(\frac{r}{r_o})\right]$$

$$A_2(r) = -\frac{r_o^4}{16}\left[\frac{5}{4} - (\frac{r}{r_o})^2 - \frac{1}{4}(\frac{r}{r_o})^4 + (1 + 2(\frac{r}{r_o})^2)\ln(\frac{r}{r_o})\right]$$

$$A_3(r) = \frac{r_o^6}{64}\left[\frac{10}{36} + \frac{1}{4}(\frac{r}{r_o})^2 - \frac{1}{2}(\frac{r}{r_o})^4 - \frac{1}{36}(\frac{r}{r_o})^6 + (\frac{1}{6} + (\frac{r}{r_o})^2 + \frac{1}{2}(\frac{r}{r_o})^4)\ln(\frac{r}{r_o})\right]$$

$$\tag{6b}$$

and that of $B_n(r)$ are ;                              (

$$B_o(r) = -r_o \ln(\frac{r}{r_o}) ,$$

$$B_1(r) = \frac{r_o^3}{4}\left[ 1 - (\frac{r}{r_o})^2 + (1+(\frac{r}{r_o})^2)\ln(\frac{r}{r_o}) \right]$$

$$B_2(r) = -\frac{r_o^5}{64}\left[ \frac{3}{2} - \frac{3}{2}(\frac{r}{r_o})^4 + (1+4(\frac{r}{r_o})^2+(\frac{r}{r_o})^4)\ln(\frac{r}{r_o}) \right]$$

$$B_3(r) = \frac{r_o^7}{128}\left[\frac{11}{108} + \frac{1}{4}(\frac{r}{r_o})^2 - \frac{1}{4}(\frac{r}{r_o})^4 - \frac{11}{108}(\frac{r}{r_o})^6 + \right.$$
$$\left. (\frac{1}{18} + \frac{1}{2}(\frac{r}{r_o})^2 + \frac{1}{2}(\frac{r}{r_o})^4 + \frac{1}{18}(\frac{r}{r_o})^6)\ln(\frac{r}{r_o}) \right]$$

$$\qquad (6c)$$

Combining Eqs. (2), (5) and (6) gives the temperature field :

$$T(r,y) = \left[T_o(y) - \frac{r_o}{k}\ln(\frac{r}{r_o})q_o(y)\right] + \frac{\overset{*}{q}r_o^2}{4k}\left[1 - (\frac{r}{r_o})^2 + \ln(\frac{r}{r_o})^2\right] +$$
$$\sum_{n=1}^{\infty} A_n(r) \frac{d^{2n}T_o(y)}{dy^{2n}} + \frac{1}{k}\sum_{n=1}^{\infty}B_n(r)\frac{d^{2n}q_o(y)}{dy^{2n}} \qquad (7)$$

It is important to note from the right-hand side of Eq. (7) that the terms inside the brackets represent a steady, one-dimensional solution in the radial direction. The effect of two-dimensional heat transfer is included in the remaining terms. It is also important to state that in carrying out the analysis, no reference was made to the axial-boundary conditions at the two planes (r,0) and (r,L). However, this omission is no cause for concern. Because of the smooth nature of the linear governing differential equation, the temperature distribution T(r,0) and T(r,L) is uniquely specified when the temperature and its exterior radial derivatives outside the surface of the cylinder are known in the interval : $0 \le y \le L$ .

## 2.2 ANALYSIS OF PROBLEM (1b)

If the two boundary conditions used in the above analysis are prescribed at the inner surface of the hollow cylinder instead of the outer surface, as it is shown in Fig. 1b, the solution becomes

$$T(r,y) = \left[T_i(y) - \frac{r_i}{k}\ln(\frac{r}{r_i})q_i(y)\right] + \frac{\overset{*}{q}r_i^2}{4k}\left[1 - (\frac{r}{r_i})^2 + \ln(\frac{r}{r_i})^2\right] +$$
$$\sum_{n=1}^{\infty} f_n(r)\frac{d^{2n}T_i(y)}{dy^{2n}} + \frac{1}{k}\sum_{n=1}^{\infty}g_n(r)\frac{d^{2n}q_i(y)}{dy^{2n}} \qquad (8a)$$

where $T_i(y) = T(r_i,y)$ and $q_i(y) = q_r(r_i,y)$ are the inner surface temperature and heat flux, respectively, which should be known

continuous and differentiable functions of the axial coordinate y.
The leading terms of the r-dependent coefficients $f_n(r)$ are :

$$f_0(r) = 1, \quad f_1(r) = \frac{r_i^2}{4}\left[1 - (\frac{r}{r_i})^2 + 2\ln(\frac{r}{r_i})\right]$$

$$f_2(r) = -\frac{r_i^4}{16}\left[\frac{5}{4} - (\frac{r}{r_i})^2 - \frac{1}{4}(\frac{r}{r_i})^4 + (1+2(\frac{r}{r_i})^2)\ln(\frac{r}{r_i})\right]$$

$$f_3(r) = \frac{r_i^6}{64}\left[\frac{10}{36} + \frac{1}{4}(\frac{r}{r_i})^2 - \frac{1}{2}(\frac{r}{r_i})^4 - \frac{1}{36}(\frac{r}{r_i})^6 + \right.$$
$$\left. (\frac{1}{6} + (\frac{r}{r_i})^2 + \frac{1}{2}(\frac{r}{r_i})^4)\ln(\frac{r}{r_i})\right]$$

(8b)

and that of $g_n(r)$ are :

$$g_0(r) = -r_i\ln(\frac{r}{r_i}),$$

$$g_1(r) = \frac{r_i^3}{4}\left[1 - (\frac{r}{r_i})^2 + (1+(\frac{r}{r_i})^2)\ln(\frac{r}{r_i})\right]$$

$$g_2(r) = -\frac{r_i^5}{64}\left[\frac{3}{2} - \frac{3}{2}(\frac{r}{r_i})^4 + (1+4(\frac{r}{r_i})^2+(\frac{r}{r_i})^4)\ln(\frac{r}{r_i})\right]$$

(8c)

$$g_3(r) = \frac{r_i^7}{128}\left[\frac{11}{108} + \frac{1}{4}(\frac{r}{r_i})^2 - \frac{1}{4}(\frac{r}{r_i})^4 - \frac{11}{108}(\frac{r}{r_i})^6 + \right.$$
$$\left. (\frac{1}{18} + \frac{1}{2}(\frac{r}{r_i})^2 + \frac{1}{2}(\frac{r}{r_i})^4 + \frac{1}{18}(\frac{r}{r_i})^6)\ln(\frac{r}{r_i})\right]$$

## 3. TEST EXAMPLE AND DISCUSSION

In the above section, general solution for  the stated inverse
problem has been derived. At this point   it is informative to
consider test problems having known exact solutions in order to
prove validity of the proposed solution   as well to bring the
features of the method  in more detail. Since there is no another
method available  to solve this kind of the dealt inverse problems,
therefore, no such a typical inverse  problem with known exact
solution is available to us to be used as test problem. Therefore,
we will construct a direct problem and then  find its exact solution
which  will  be  used  to  construct  an  inverse  test  problem
corresponding to the dealt problem.

As first step to perform  this task, we set the direct problem :
Consider a hollow cylinder  of constant thermal conductivity and
involving uniform internal heat generation. The outer surface is
exposed to heat losses of constant heat flux $q_o$, while the inner
surface temperature profile is given by  $T(r_i, y) = T_a - T_b \cos(\omega y)$;
$\omega = \pi/L$. The cylinder wall are insulated at both axial ends.

The solution of the above problem, derived in Appendix (I), is

$$T(r,y)=T_a - T_b\cos(\omega y) \; D(\omega r)+\frac{q_o r_o}{k}\ln(\frac{r_i}{r})+\frac{\overset{*}{q}r_o^2}{4k}\left[\ln(\frac{r}{r_i})^2-(\frac{r}{r_o})^2+(\frac{r}{r_o})^2\right] \qquad (9)$$

where $\overset{*}{q}$ is the volumetric heat generation rate, and $D(\omega r)$ is r-dependent function defined by Eq. (18) in Appendix (I).

Now, with help of the above exact solution we construct the following inverse problem :

$$q_o(y) = q_o \quad (\text{constant}) \qquad\qquad\qquad\qquad (10a)$$

$$T_o(y) = T(r_o,y), \text{ (calculated by Eq. (9) with } r = r_o) \qquad (10b)$$

The above inverse problem is corresponding to problem (1a). The general solution, given by Eq. (6a), under the boundary conditions (10a, b) becomes :

$$T(r,y)=\left[T(r_o,y)-\frac{r_o q_o}{k}\ln(\frac{r}{r_o})\right]+\frac{\overset{*}{q}r_o^2}{4k}\left[1-(\frac{r}{r_o})^2+\ln(\frac{r}{r_o})^2\right]+\sum_{n=1}^{N}A_n(r)\frac{d^{2n}T(r_o,y)}{dy^{2n}} \qquad (11)$$

where N is the upper limit number of the truncated series, which is integer number $\le 4$. The terms of $A_n(n)$ are given by Eq. (6b). The outer surface temperature and its y derivatives are calculated by Eq. (9); with $r = r_o$.

For purpose of the method testing, we will compare present solution results, calculated by Eq. (11), with the corresponding exact results from Eq. (9). Examples of such comparisons for radial distribution of temperature, and radial heat flux are presented in Figs. 2a and 3a, respectively. The data used in these comparisons are : $r_i=.01$ m, $r_o/r_i=2$, $L/r_o=4$, $q_r(r_o)=q_o=70$ kW/m$^2$, $k=0.38$ kW/(m$^2$k), $T_a=400°C$, $T_b=200°C$ and $\overset{*}{q}= 4.9 \times 10^5$ W/m$^3$.

It is evident from Figs. 2a and 3a that the present results of N=1 for radial profiles of temperature and radial heat flux, respectively, (represented by symbols in graphs) have small deviations from the corresponding exact results (full lines). It is more evident in Figs. 2b and 3b that the relative error in the present results is zero at the input-data boundary surface (ie, the outer surface) and increases with distance therefrom to reach maximum value at the inner surface. It is also noted that the error in the heat flux results are greater than that in the temperature results. However, the present results with N=2 in eq. (11) are very accurate and indistinguishable from the exact solution; both are indicated by full lines in Figs. 2a and 3a.

From the notion that the accuracy of present solution results of N=1 decreases with distance from the outer boundary surface (cf, Figs. 2b and 3b), one may deduce that the geometric dimensions of the cylinder have an effect on the accuracy of the present solution of a truncated series.
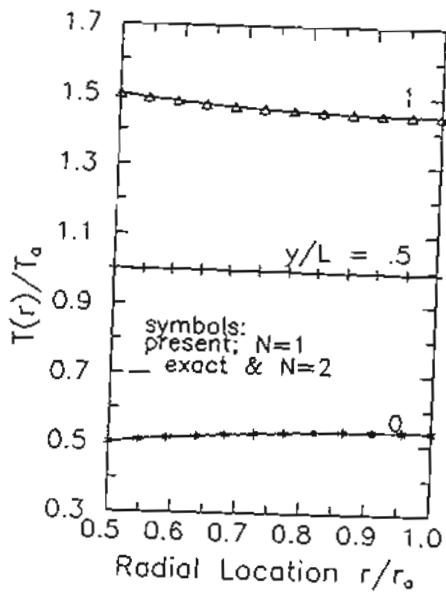
Fig. 2a Comparison of exact and present results for radial temperature distribution
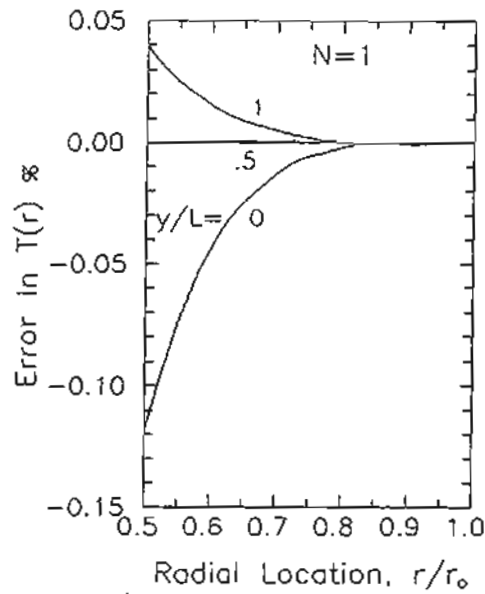
Fig. 2b The accuracy of present results; by Eq. (11) with N=1, for radial temperature profiles depicted in Fig.2 by symbols.
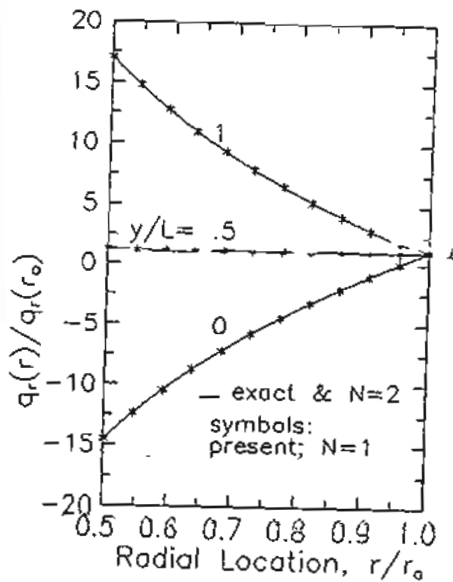


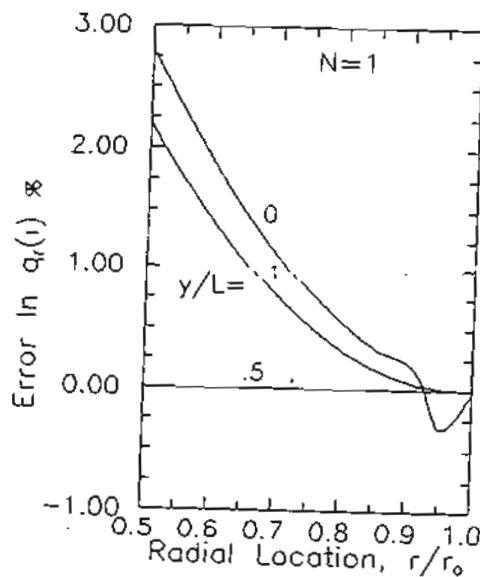Fig. 3a Comparison of exact and present results for radial heat flux distribution

Fig. 3b The accuracy of present results; by Eq. (11) with N=1, for radial heat heat flux profiles depicted in Fig. 3a by symbols

To investigate the effect of the geometric dimensions of the hollow cylinder on the accuracy of the present solution, results with N=1 and N=2 are presented in Figs. 4a and 4b, respectively. These results are plotted in terms of the maximum absolute error in temperatures, calculated by Eq. (11), versus the radius ratio $r_o/r_i$;

for three different values of the dimensionless length $L/r_o$. Figure 4a displays that for long cylinders ($L/r_o \geq 8$) of thick or thin wall, the solution of truncated series of N=1 is adequate, but not appropriate for thick-walled    short cylinders with $L/r_o \leq 2$. However, with increasing number of terms in the truncated series from N=1 to    N=2, the error rapidly dimensions to be insignificant (cf, Fig. 4b)  for short and long cylinders of radius ratio $r/r_o \leq 3$

The results in Figs. 4a and 4b are calculated using the same data set used for Figs. 2 and 3.

Figure 5a shows comparison of exact and present results  for two axial temperature profiles with low, and steep axial variation introduced in the graphs  by case 1 and case 2, respectively. It is clear that the present results of  N = 2 for both cases are very exact and indistinguishable from the corresponding exact results (full lines). However, the accuracy of the present results of N = 1 in case 2  is lower  than  that in case 1. as it is clear in Fig. 5b. This proves that the present method  is capable to accommodate boundary conditions functions of sharp axial variation.

Here, it is important to point out that the present  method may be of a considerable practical interest, however, to some steady heat transfer experiments using a circular   test tube    with significant axial variation in wall temperature and/or heat flux owing to the nature of the   studied phenomenon. In many of such experiments,   it is  desirable  to  estimate  the 2-dimensional temperature field of tube wall in order to calculate accurately the heat flux and temperature at the inner tube surface from only some corresponding measurements at the   outer surface.  For this task, the present approach may be used, however, if  two  boundary conditions   at the outer  surface of the tube, gained from the measurements, fall in one of the following classifications :

a) the axial  distribution  of  temperature and  that  of  heat flux outside the tube surface  are known.
b) convective heating or  cooling of constant   heat transfer coefficient at the outer  surface of temperature varies with the axial  location.
c) insulated surface  of   known   axial   temperature profile.
d) isothermal surface  of known axial heat flux  distribution.

Case (a) represents the general feature of the dealt problem of Fig. 1a, as well indirectly is case (b), whereas case (c) and case (d) bring out  the problem in simplified features.

However, in such a practical situation  the measured data are not given  by  such  convenient  analytical  expressions used  in  the theoretical treatment, but as data measured at  some  different  axial locations.  Therefore, it  is  customary  to  represent  these  data analytically by a fit formula (as  polynomial) using the method of least squares. Then, this fit formula can be  used to calculate the axial-derivative terms in the series of the solution. An alternative
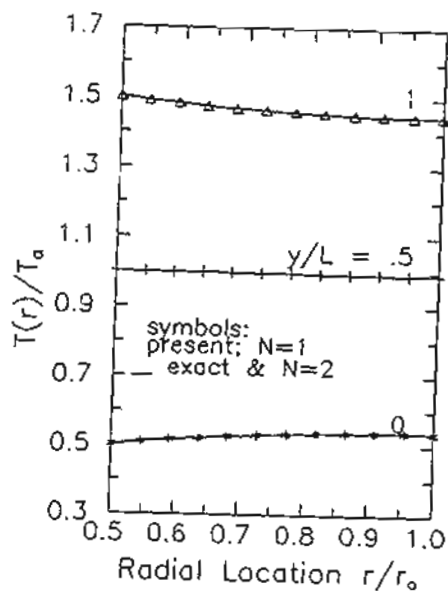
Fig. 2a Comparison of exact and
present results for radial
temperature distribution

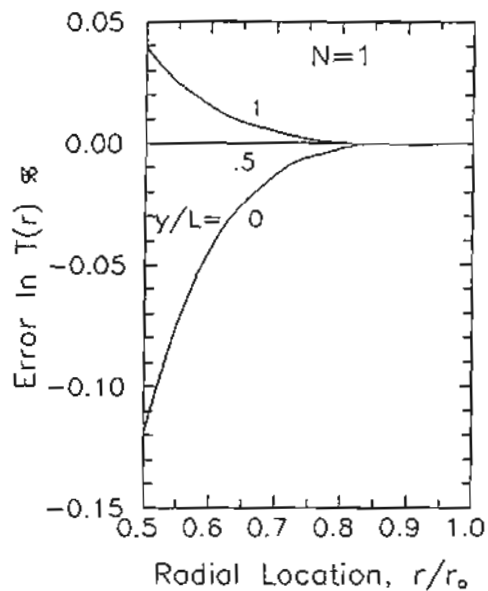Fig. 2b The accuracy of present
results; by Eq. (11) with
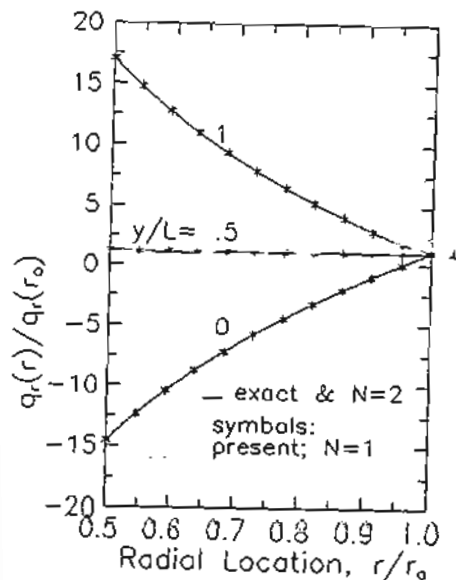N=1, for radial temperature
profiles depicted in Fig.2
by symbols.

Fig. 3a Comparison of exact and
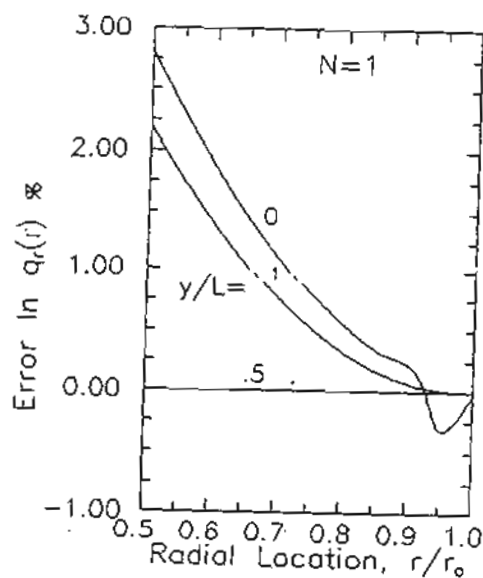present results for radial
heat flux distribution

Fig. 3b The accuracy of present
results; by Eq. (11) with
N=1, for radial heat
heat flux profiles
depicted in Fig. 3a
by symbols

To investigate the effect of the geometric dimensions of the hollow cylinder on the accuracy of the present solution, results with N=1 and N=2 are presented in Figs. 4a and 4b, respectively. These results are plotted in terms of the maximum absolute error in temperatures, calculated by Eq. (11), versus the radius ratio $r_o/r_i$; for three different values of the dimensionless length $L/r_o$. Figure 4a displays that for long cylinders ($L/r_o \geq 8$) of thick or thin wall, the solution of truncated series of N=1 is adequate, but not appropriate for thick-walled short cylinders with $L/r_o \leq 2$. However, with increasing number of terms in the truncated series from N=1 to N=2, the error rapidly dimensions to be insignificant (cf, Fig. 4b) for short and long cylinders of radius ratio $r/r_o \leq 3$ The results in Figs. 4a and 4b are calculated using the same data set used for Figs. 2 and 3.

Figure 5a shows comparison of exact and present results for two axial temperature profiles with low, and steep axial variation introduced in the graphs by case 1 and case 2, respectively. It is clear that the present results of N = 2 for both cases are very exact and indistinguishable from the corresponding exact results (full lines). However, the accuracy of the present results of N = 1 in case 2 is lower than that in case 1, as it is clear in Fig. 5b. This proves that the present method is capable to accommodate boundary conditions functions of sharp axial variation.

Here, it is important to point out that the present method may be of a considerable practical interest, however, to some steady heat transfer experiments using a circular test tube with significant axial variation in wall temperature and/or heat flux owing to the nature of the studied phenomenon. In many of such experiments, it is desirable to estimate the 2-dimensional temperature field of tube wall in order to calculate accurately the heat flux and temperature at the inner tube surface from only some corresponding measurements at the outer surface. For this task, the present approach may be used, however, if two boundary conditions at the outer surface of the tube, gained from the measurements, fall in one of the following classifications :

a) the axial distribution of temperature and that of heat flux outside the tube surface are known.
b) convective heating or cooling of constant heat transfer coefficient at the outer surface of temperature varies with the axial location.
c) insulated surface of known axial temperature profile.
d) isothermal surface of known axial heat flux distribution.

Case (a) represents the general feature of the dealt problem of Fig. 1a, as well indirectly is case (b), whereas case (c) and case (d) bring out the problem in simplified features.

However, in such a practical situation the measured data are not given by such convenient analytical expressions used in the theoretical treatment, but as data measured at some different axial locations. Therefore, it is customary to represent these data analytically by a fit formula (as polynomial) using the method of least squares. Then, this fit formula can be used to calculate the axial-derivative terms in the series of the solution. An alternative
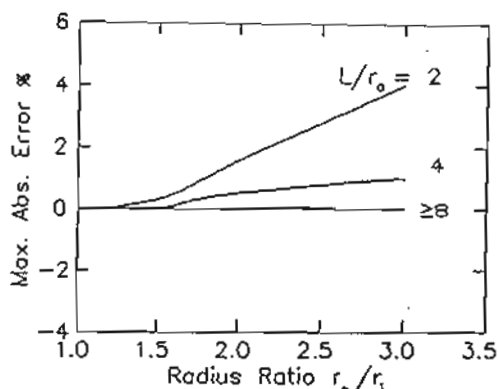
Fig. 4a Effect of the geometric
         dimensions ratios on the
         accuracy of results from
         the present solution of
         truncated-series with N=1



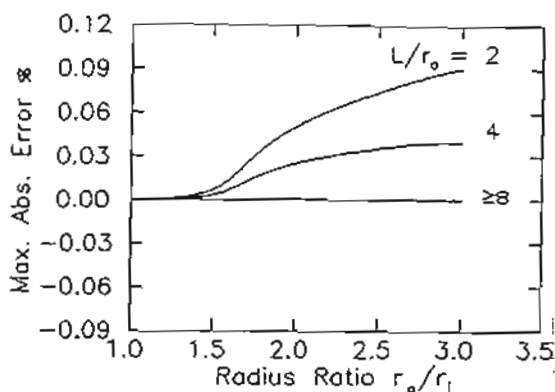Fig. 4b Effect of the geometric
         dimensions ratios on the
         accuracy of results from
         the present solution of
         truncated-series with N=2
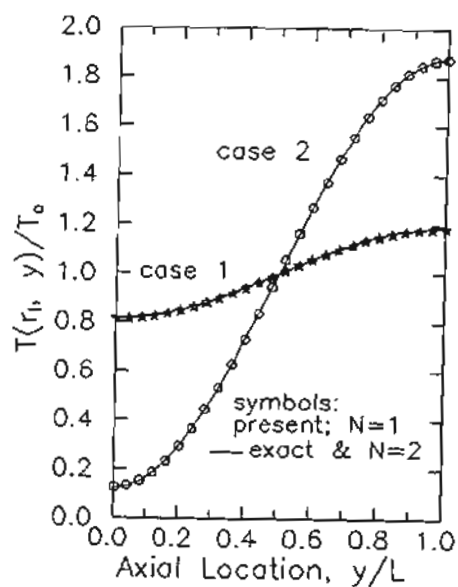


Fig. 5a Comparison of exact and
         present results for two
         different cases of axial
         temperature distribution :
         case 1: low axial variation;
         $T_a = 400\,^\circ C$, $T_b = 50\,^\circ C$ in Eq.(11)
         case 2: steep axial variation;
         $T_a = 400\,^\circ C$, $T_b = 350\,^\circ C$ in Eq.(11)



Fig. 5b The accuracy of present
         results; by Eq. (11) with
         N=1, for the two types
         of the axial temperature
         profile depicted in Fig. 5a
         by symbols

way is to calculate  these derivatives numerically direct from measured data interpolated at discrete axial points by an interpolating procedure such as Spline procedure. Thus, the axial temperature derivatives at a certain axial point on the outer tube sur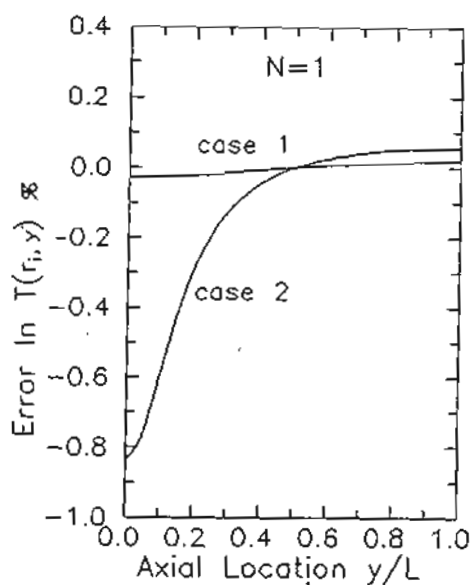face can be approximated numerically [10]. This numerical calculation of the derivative terms has the advantage that the magnitude of the highest derivative retained in the series of the solution may be monitored. Thus a check on the validity of the truncated-series solution is available [12].

## 4. MAIN POINTS

1- The prerequisites for the theoretical application of the method are that the axial distribution for each the temperature and heat flux at the outer or the inner surface of a hollow cylinder  are known  continuous              and differentiable functions of the axial coordinate.

2- The solution is explicit, exact and capable to accommodate boundary conditions data of sharp axial variation.

3- The effect of internal heat generation is  exactly modeled.

4- The  accuracy of a truncated-series solution depends on  the geometric  dimensions ratio, number of terms in the truncated series and the  axial  variation degree in   the utilized boundary data.

5- The method may also be  considered  of  a practical  interest.


APPENDIX (I)

With reference to  the geometry and coordinates system of Fig. 1, the direct problem, presented in section 3, can be described by

$$\frac{\partial^2 T}{\partial r^2} + \frac{1}{r}\frac{\partial T}{\partial r} + \frac{\partial^2 T}{\partial y^2} + \frac{\overset{*}{q}}{k} = 0 \tag{12a}$$

$$\left.\frac{\partial T}{\partial r}\right|_{r_o} = -\frac{q_o}{k}, \tag{12b} \qquad T(r_i,y) = T_a - T_b \cos(\omega y), \tag{12c}$$

$$\left.\frac{\partial T}{\partial y}\right|_{y=0} = 0, \tag{12d} \qquad \left.\frac{\partial T}{\partial y}\right|_{y=L} = 0. \tag{12e}$$

where $T_a$ and $T_b$ are known constant temperatures, and $\omega = \pi/L$.

By the principle of superposition, solution of problem (12) may be assumed :

$$T(r,y) = \Theta_2(r,y) + \Theta_1(r) \tag{13}$$

Here, $\Theta_1(r)$ is assumed to satisfy the one-dimensional problem :

$$\frac{d^2\Theta_1}{dr^2} + \frac{1}{r}\frac{d\Theta_1}{dr} + \frac{\overset{*}{q}}{k} = 0, \qquad \left.\frac{d\Theta_1}{dr}\right|_{r_o} = -\frac{q_o}{k}, \qquad \Theta_1(r_i) = 0. \tag{14}$$

The solution of  the above problem is :

$$\Theta_1(r) = \frac{q_o r_o}{k} \ln(r_i/r) + \frac{\overset{*}{q} r_o^2}{4k}\left[\ln(r/r_i)^2 - (r/r_o)^2 + (r_i/r_o)^2\right] \tag{15}$$

From combining Eqs. (12)-(14), we fined $\Theta_2(r,y)$ is satisfied by

$$\frac{\partial^2 \Theta_2}{\partial r^2} + \frac{1}{r}\frac{\partial \Theta_2}{\partial r} + \frac{\partial^2 \Theta_2}{\partial y^2} = 0, \tag{16a}$$

$$\left.\frac{\partial \Theta_2}{\partial r}\right|_{r_o} = 0 \qquad (16b), \qquad \Theta_2(r_i,y) = T_a - T_b \cos(\omega y) \qquad (16c)$$

$$\left.\frac{\partial \Theta_2}{\partial y}\right|_{y=0} = 0, \qquad (16d), \qquad \left.\frac{\partial \Theta_2}{\partial y}\right|_{y=L} = 0 \tag{16e}$$

The solution of the above problem can be obtained by applying the method of variables separation [12], which is :

$$\Theta_2(r,y) = T_a - T_b \cos(\omega y) \propto(\omega r) \tag{17}$$

where $\propto(\omega r) = \left[\dfrac{I_o(\omega r)K_1(\omega r) + I_1(\omega r)K_o(\omega r)}{I_o(\omega r_i)K_1(\omega r_o) + I_1(\omega r_o)K_o(\omega r_i)}\right]$ \hfill (18)

Combining Eqs. (13), (15) and (17) gives the temperature field :

$$T(r,y) = T_a - T_b\cos(\omega y) \propto(\omega r) + \frac{q_o r_o}{k}\ln(\frac{r_i}{r}) + \frac{\overset{*}{q}r_o}{4k}\left[\ln(\frac{r}{r_i})^2 - (\frac{r}{r_o})^2 + (\frac{r_i}{r_o})^2\right] \tag{19}$$

NOMENCLATURE

| | |
|---|---|
| $B_1, B_2, C_1, C_2$ | constants, dimensionless |
| $I_o, I_1$ | modified Bessel functions of the first kind, dimensionless |
| $k$ | thermal conductivity, $kW/(m\,^oC)$ |
| $k_o, k_1$ | modified Bessel functions of the second kind, dimensionless |
| $L$ | cylinder length, m |
| $q$ | heat flux, $kW/m^2$ |
| $q_o(y)$ | radial heat flux at the outer surface $(=q_r(r_o,y))$, $kW/m^2$ |
| $q_i(y)$ | radial heat flux at the inner surface $(=q_r(r_i,y))$, $kW/m^2$ |
| $N$ | the upper limit number of the truncated series, dimensionless |
| $r$ | radial coordinate, m |
| $r_o$ | outer cylinder radius, m |

| | |
|---|---|
| $r_i$ | inner cylinder radius, m |
| $A_n(r)$, $f_n(r)$ | r-dependent coefficients, $m^{2n}$ |
| $B_n(r)$, $g_n(r)$ | r-dependent coefficients, $m^{2n+1}$ |
| $T$ | temperature, $^oC$ |
| $T_a$, $T_b$ | constant temperatures, $^oC$ |
| $T_o(y)$ | outer surface temperature ($=T(r_o, y)$), $^oC$ |
| $T_i(y)$ | inner surface temperature ($=T(r_i, y)$), $^oC$ |
| $y$ | axial coordinate, m |
| $\overset{*}{q}$ | volumetric heat generation rate, $kW/m^3$ |

SUBSCRIPTS:

| | |
|---|---|
| o | outer surface |
| $\iota$ | inner surface |
| r | radial direction |
| y | axial direction |

## REFERENCES

1  Mosaad  M.  .General  Exact  Inverse  Solution  To  Steady
   Two-Dimensional Heat Conduction with heat  Generation  in a Plane
   Wall, Accepted for Publication in Mansoura University Journal.
2  Beck, J.  V.,  Blackwell,  B.  and Charles,  Jr.,  Inverse  Heat
   Conduction,  1st  Ed., New York, John Wiley & Sons Inc., 1985.
3  Weber, C.F.,  Analysis  and  Solution  of  the  Ill-Posed  Inverse
   problem. Int. J. Heat Mass Transfer, 24, 1783-1792, 1981.
4  Al-Najem, N. M.  and Ozisik, M. N., Inverse Heat  Conduction in
   Composite Plane Layers. Pub. of ASME 85-Ht-53. 1985.
5  Raynaud, M. and Beck, J.V., Methodology for Comparison of Inverse
   Heat Conduction Methods. Pub. of ASME. 85-WA/HT-40. 1985.
6  Al-Najem, N. M.  and  Ozisik,  M. N.,  On  the  Solution  of
   Three-Dimensional  Inverse  Heat Conduction in Finite Media, Int.
   J. Heat Mass Transfer, 2121-2128, 1985.
7  Burggraf, O. R.,  An Exact Solution of the  Inverse  Problem  in
   Heat Conduction;  Theory and  Applications, J. of Heat  Transfer.
   86C, 373-382, 1964.
8  Barcilon, V., Iterative Solution of the  Inverse  Sturm-Liouville
   Problem. J. Math. Phys., 14. 429-436, 1984.
9  Bell, G.E.. An Inverse  Solution  for  Steady  Temperature  Field
   within a Solidified  Layer, Int.  J.  Heat  Mass  Transfer.  22,
   23331-23337, 1985.
10 Mosaad, M., On the Theory of  the  Inverse  Problem of  Steady,
   Two-Dimensional  Heat  Conduction in a Hollow  cylindrical  Wall.
   Mansoura  Eng. J. (MEJ), 17, 93-101, 1992.
11 Mosaad. M.. Inverse Problem of Steady-State, Two-Dimensional Heat
   Conduction  in  a  Hollow  Cylindrical  Wall,  Theory  and
   Applications. Accepted for Publication in  the  3rd  World
   Conference on Heat Transfer. Fluid Mechanics and  Thermodynamics.
   Honolulu. Hawaii. USA. Oct. 31-Nov. 5, 1993.
12 Mosaad. M., Analytical Solution of an Inverse Problem in  Steady,
   Two-Dimensional  Heat Conduction for a Plane Wall. Mansoura  Eng.
   J. (MEJ), 17, 58-71. 1992.